A Hybrid-Stress Finite Element For Linear Anisotropic Elasticity

by

Gerald W. Fly
The Computational Mechanics Company, Inc.
Austin, Texas

J. Tinsley Oden
The University of Texas at Austin
Austin, Texas

and

Mark L. Pearson
Softcom, Inc.
Huntsville, Alabama

Abstract. *Standard assumed displacement finite elements with anisotropic material properties perform poorly in complex stress fields such as combined bending and shear and combined bending and torsion. To address this problem, a set of three-dimensional hybrid-stress brick elements were developed with fully anisotropic material properties. Both eight-node and twenty-node bricks were developed based on the symmetry group theory of Punch and Atluri. An eight-node brick was also developed using complete polynomials and stress basis functions and reducing the order of the resulting stress parameter matrix by applying equilibrium constraints and stress compatibility constraints. Here the stress compatibility constraints must be formulated assuming anisotropic material properties. The performance of these elements was examined in numerical examples covering a broad range of stress distributions. The stress predictions show a significant improvement over the assumed displacement elements but the calculation time is increased.*

Introduction

The development of high strength single crystal metallic alloys, such as those used in the turbine blades in the fuel pump in the space shuttle main engine, has placed new emphasis on the need for anisotropic stress analysis, especially in the area of finite element analysis. These single crystal materials have a high degree of anisotropy and the use of standard assumed displacement finite elements can lead to very poor approximations of stresses, displacements, natural frequencies, and mode shapes. This work outlines the possibility of resolving these deficiencies by developing hybrid stress elements formulated for three dimensional linear anisotropic elasticity.

The hybrid stress elements are based upon a modified complementary energy principle in which the displacements and stresses are independently interpolated. Two approaches to the interpolations are considered here, both of which assure correct stiffness rank, coordinate invariance, and elimination of spurious zero energy modes. The first is based on work by Spilker, Maskeri, and Kania [1] and Spilker and Singh [2] in which complete equilibrated polynomials are used. The number of stress parameters is reduced by applying compatibility constraints reformulated in terms of the stresses. The second approach is based upon recent work by Rubenstein, Punch and Atluri [3] and Punch and Atluri [4, 5] in which group theoretical methods are used to minimize the number of stress parameters while still satisfying rank and invariance requirements.

Eight node and 20 node brick elements have been compared to both standard displacement elements and to exact solutions, when possible, for both isotropic and anisotropic materials. These comparisons have been made on single elements as well as on multielement cantilever beams under various loading conditions. The hybrid elements have demonstrated significantly improved performance for the analysis of highly anisotropic materials. In fact, eight node hybrid elements have shown superior performance to 20 node displacement elements where the material is highly anisotropic.

1 Derivation of the Element Stiffness Matrix

The hybrid stress model is developed in the same manner regardless of the form of stress interpolation. The development is based upon a modified complimentary energy principle in which Lagrange multipliers are used to relax interelement traction continuity and mechanical boundary conditions. The required functional for the hybrid stress formulation is given by:

$$\Pi_{mc} = \sum_n \left\{ \frac{1}{2} \int_{V_n} \sigma^T s \sigma dV - \int_{V_n} \sigma^T (Du) dV + \int_{S\sigma n} u^T \overline{T} dS \right\} \qquad (1.1)$$

where σ is the stress vector, S is the compliance matrix for the material, D is the strain–displacement matrix, u represents the local displacements, and $\overline{T}$ are the prescribed traction boundary conditions.

The local displacements are interpolated in terms of the nodal displacements through the displacement shape functions N.

$$\begin{aligned} u &= \sum N_i(\xi,\ \eta,\ \zeta)u_i \\ v &= \sum N_i(\xi,\ \eta,\ \zeta)v_i \\ w &= \sum N_i(\xi,\ \eta,\ \zeta)w_i \end{aligned} \tag{1.2}$$

where u_i, v_i and w_i represent the displacements at node i. Equations (1.2) can be expressed more concisely in matrix form as

$$u = Nq \tag{1.3}$$

where q is a column vector of the nodal displacements. The displacement shape functions used for these three dimensional elements are the serendipity shape functions. The same shape functions are used to map the actual element geometry into the master element coordinate system generating standard isoparametric elements in terms of displacements. The coordinate transformation is given by

$$\begin{aligned} x &= \sum N_i(\xi,\ \eta,\ \zeta)x_i \\ y &= \sum N_i(\xi,\ \eta,\ \zeta)y_i \\ z &= \sum N_i(\xi,\ \eta,\ \zeta)z_i \end{aligned} \tag{1.4}$$

The strains are related to the displacements in exactly the same manner as for a standard assumed displacement technique. The strain displacement matrix D is then given by

$$D = \begin{bmatrix} \partial/\partial x & 0 & 0 \\ 0 & \partial/\partial y & 0 \\ 0 & 0 & \partial/\partial z \\ \partial/\partial y & \partial/\partial x & 0 \\ \partial/\partial z & \partial/\partial z & \partial/\partial y \end{bmatrix} \tag{1.5}$$

and the local strains are given by

$$\hat{\epsilon} = Du = DNq = Bq \tag{1.6}$$

The stresses are interpolated separately from the displacements using a different set of interpolation functions. In addition, rather than interpolating in terms of the nodal displacements, the stresses are interpolated in terms of a set of stress parameters β which are only indirectly related to the nodal

displacements. The stresses σ are related to these stress parameters via the stress interpolation function matrix P:

$$\sigma = P(x, y, z)\beta \tag{1.7}$$

such that the homogeneous equilibrium conditions are exactly satisfied, i.e.,

$$E\sigma = EP\beta = 0 \tag{1.8}$$

Substituting (1.7) into (1.1) yields

$$\Pi_{mc} = \sum_n \left\{ \frac{1}{2} \int_v \beta^T P^T S P \beta dV - \int_v \beta^T P^T B q dV + \int_{S_{\sigma n}} q^T N^T \overline{T} dS \right\} \tag{1.9}$$

The differential volume dV can be found in terms of the determinant of the Jacobian of the coordinate transformation as

$$dV = |J| d\xi d\eta d\zeta \tag{1.10}$$

The following element matrices can be defined from equations (1.9) and (1.10) to simplify statement of the complimentary energy function

$$\begin{aligned} H &= \int_{-1}^{1} \int_{-1}^{1} \int_{-1}^{1} P^T S P |J| d\xi d\eta d\zeta \\ G &= \int_{-1}^{1} \int_{-1}^{1} \int_{-1}^{1} P^T B |J| d\xi d\eta d\zeta \\ Q &= \int_{S\sigma n} N^T \overline{T} dS \end{aligned} \tag{1.11}$$

The element degrees of freedom are related to the global degrees of freedom by the matrix L

$$q = Lq^* \tag{1.12}$$

Substituting equations 1.11–1.16 into equation 1.9 yields:

$$\Pi_{mc} = \sum_n \left\{ \frac{1}{2} \beta^T H \beta - \beta^T G L q^* + q^{*T} L Q \right\} \tag{1.13}$$

Taking the first variation of Π_{mc} with respect to β and setting the variation to zero gives:

$$(H\beta - GLq^*)\delta\beta = 0 \tag{1.14}$$

$$\beta = H^{-1} G L q^* \tag{1.15}$$

Substituting this definition for β back into Π_{mc} yields:

$$\begin{aligned} \Pi_{mc} &= \sum_n \left\{ \frac{1}{2} q^{*T} L^T G^T H^{-1} G L q^* - q^{*T} L^T G^T H^{-1} G L L q^* + q^{*T} L^T Q \right\} \\ &= \sum_n \left\{ -\frac{1}{2} q^{*T} L^T G^T H^{-1} G L q^* + q^{*T} L^T Q \right\} \end{aligned} \tag{1.16}$$

Setting the first variation of Π_{mc} with respect to q to zero, we obtain

$$\begin{gathered}\left(-L^T G^T H^{-1} G L q^* + L^T Q\right) \delta q^* = 0 \\ L^T K L q^* = L^T Q\end{gathered} \tag{1.17}$$

where $K = G^T H^{-1} G$ and is the element stiffness matrix and Q is the forcing vector due to surface tractions.

2 Formulation of the Assumed Stress Field

The assumed stress field must satisfy the homogeneous equilibrium equations, must provide an element stiffness matrix with no spurious zero energy modes, and must be invariant under rotation. The number of stress parameters must be greater than or equal to the number of element degrees of freedom minus the number of rigid body modes for the stiffness matrix to be of sufficient rank to eliminate spurious modes. This minimum number of β's is a necessary condition but not a sufficient condition to guarantee adequate rank in the stiffness matrix, nor does a stress field which achieves adequate rank assure an element which is rotationally invariant. However, systematic approaches to defining the stress field are available which can achieve both goals.

Spilker has shown that if the stress field consists of complete polynomials (i.e., complete quadratics, or complete cubics) the resulting stiffness matrix will both be of sufficient rank and will be invariant so long as the number of β's equals or exceeds the minimum requirement. For an eight node brick, a full quadratic stress interpolation is required while for the 20 node brick the minimum complete polynomial is a cubic. The stress field for the eight node bricks is then defined as:

$$\begin{bmatrix} \sigma_x \\ \sigma_y \\ \sigma_z \\ \tau_{xy} \\ \tau_{xz} \\ \tau_{yz} \end{bmatrix} = \begin{bmatrix} p_1 & & & & & \\ & p_2 & & & & \\ & & p_3 & & & \\ & & & p_4 & & \\ & & & & p_5 & \\ & & & & & p_6 \end{bmatrix} \begin{bmatrix} \beta_1 \\ \cdot \\ \cdot \\ \cdot \\ \cdot \\ \beta_{60} \end{bmatrix} \tag{2.18}$$

where the p_i's are row vectors of length 10. Thus

$$\sigma_x = \beta_1 + 2\beta_2 x + 2\beta_4 z + \beta_5 x^2 + 2\beta_6 xy + 2\beta_7 xz + \beta_8 y^2 + 2\beta_9 yz + \beta_{10} z^2 \tag{2.19}$$

A total of 60 β's are required to initially define the stress field, but when equilibrium constraints are applied, twelve of these stress parameters are eliminated. To further reduce the number of stress parameters, the following

strain compatibility conditions are applied:

$$\begin{aligned}
&\frac{\partial^2\epsilon_x}{\partial y^2}+\frac{\partial^2\epsilon_y}{\partial x^2}=\frac{\partial^2\gamma_{xy}}{\partial x\partial y} \qquad 2\frac{\partial^2\epsilon_x}{\partial y\partial z}=\frac{\partial}{\partial x}\left(-\frac{\partial\gamma_{yz}}{\partial x}+\frac{\partial\gamma_{xz}}{\partial y}+\frac{\partial\gamma_{xy}}{\partial z}\right)\\
&\frac{\partial^2\epsilon_z}{\partial x^2}+\frac{\partial^2\epsilon_x}{\partial z^2}=\frac{\partial^2\gamma_{xz}}{\partial y\partial z} \qquad 2\frac{\partial^2\epsilon_y}{\partial z\partial x}=\frac{\partial}{\partial y}\left(\frac{\partial\gamma_{yz}}{\partial x}-\frac{\partial\gamma_{xz}}{\partial y}+\frac{\partial\gamma_{xy}}{\partial z}\right) \qquad (2.20)\\
&\frac{\partial^2\epsilon_z}{\partial x^2}+\frac{\partial^2\epsilon_x}{\partial z^2}=\frac{\partial^2\gamma_{xz}}{\partial x\partial z} \qquad 2\frac{\partial^2\epsilon_z}{\partial x\partial y}=\frac{\partial}{\partial z}\left(\frac{\partial\gamma_{yz}}{\partial x}+\frac{\partial\gamma_{xz}}{\partial y}-\frac{\partial\gamma_{xy}}{\partial z}\right)
\end{aligned}$$

For a fully anisotropic material, the strains are defined in terms of the components of the compliance matrix as:

$$\epsilon_x = a_{11}\sigma_x + a_{12}\sigma_y + a_{13}\sigma_z + a_{14}\tau_{xy} + a_{15}\tau_{xz} + a_{16}\tau_{yz} \qquad (2.21)$$

where the σ's are defined as in (1.18) above. Applying the first compatibility constraint yields

$$\begin{aligned}
&\frac{\partial^2}{\partial y^2}(a_{11}\sigma_x + a_{12}\sigma_y + a_{13}\sigma_z + a_{14}\tau_{xy} + a_{15}\tau_{xz} + a_{16}\tau_{yz})\\
&+\frac{\partial}{\partial x^2}(a_{12}\sigma_x + a_{22}\sigma_y + a_{23}\sigma_z + a_{24}\tau_{xy} + a_{25}\tau_{xz} + a_{26}\tau_{yz}) \qquad (2.22)\\
&-\frac{\partial^2}{\partial x\partial y}(a_{14}\sigma_x + a_{24}\sigma_y + a_{34}\sigma_z + a_{44}\tau_{xy} + a_{45}\tau_{xz} + a_{46}\tau_{yz}) = 0
\end{aligned}$$

Carrying out the differentiation on the equilibrated stress field yields

$$\begin{aligned}
&a_{11}(\beta_4)+a_{12}(-\beta_{47}+a_{13}(\beta_{18}+a_{14}(\beta_{26})+a_{15}(\beta_{36})+a_{16}(\beta_{46})\\
&+a_{12}(-\beta_{35})+a_{22}(\beta_{10}+a_{23}(\beta_{16}+a_{24}(\beta_{23})+a_{25}(\beta_{33})+a_{26}(\beta_{43}) \qquad (2.23)\\
&-(a_{14}(-\beta_{26})+a_{24}(-\beta_{23})+a_{34}(\beta_{17})+a_{44}(\beta_{24})+a_{45}(\beta_{34})+a_{46}(\beta_{14}))=0
\end{aligned}$$

Each equation can be used to eliminate a single β so that the resulting stress field contains 42 stress parameters.

The same procedure can be applied to the 20 node brick except that since the polynomials are cubics, the resulting equations will be functions of x, y, and z. Since these compatibility constraints must be independent of position, each of these coefficients can be equated to zero yielding a total of 24 equations. Three of these equations are dependent so that a total of 21 β's may be eliminated. Starting with a full cubic stress field with 120 β's and eliminating 30 stress parameters via the equilibrium constraints and an additional 21 parameters via the compatibility constraints produces a stress field with 69 β's.

An alternative approach to the stress field is based upon the work of Punch and Atluri. The element is formulated as a cube and due to its symmetry, it is invariant to certain rotational and reflective transformations. The

symmetry group of a cube comprises a total of 24 invariant transformations consisting of one identity transformation, nine rotations, six reflections, and eight rotation-reflections. This symmetry group has five irreducible representations. The displacement field for a 20 node brick consists of incomplete quadratics. This displacement field can be rearranged into a set of subspaces which are invariant under the symmetry group operations and these subspaces are projected onto natural irreducible invariant displacement subspaces, producing a total of 54 strain subspaces. By the same procedure the complete equilibrated stress field is decomposed into a set of 90 irreducible, invariant stress subspaces.

At this point, the stress field is precisely equivalent to the equilibrated stress field produced above. However, since each stress subspace is invariant, the removal of any stress subspace does not alter the invariance of the resulting stress field. An invariant least order stress field can be constructed from any 54 of these stress subspaces. A total of 384 choices exist for the least order stress field. While the resulting stress fields are invariant and form stiffness matrices of full rank, they are necessarily formed from incomplete polynomials and thus may not contain the cardinal stress states for pure bending, or pure torsion, etc. Several choices, though, provide excellent representation of cardinal stress states for tension, shear, bending, and torsion. Specifically the 20 node least-order selection referred to as LO20:1 by Punch and Atluri was used for these studies while the eight node selection LO8:8 was used.

The basic premise on which these elements are based is the symmetry groups for the cube. For anisotropic materials, this symmetry is clearly violated, but the resulting element is a reasonable approximation to the stress field. This same lack of symmetry applies to distorted elements but Punch and Atluri have shown that the eight node elements can tolerate mild distortions and 20 node bricks can tolerate severe distortions while still providing good results. The asymmetry due to anisotropy should have similar effects on element performance.

The elements formed from complete polynomials and reduced via equilibrium and compatibility constraints should provide superior performance for highly anisotropic materials but they also suffer in time comparisons since the number of stress parameters is so high (42 and 69 for 8 and 20 node bricks respectively).

3 Determination of the Degree of Anisotropy

A fully anisotropic material has 21 independent parameters and varying any one of these parameters changes the degree to which the materials properties differ from an isotropic material. However, to determine the influence of anisotropic material properties on the performance of these elements, it is necessary to systematically vary the material properties from an isotropic

material to a fully anisotropic material. Since very few materials exhibit full anisotropy in all orientations, it seems appropriate to begin with an orthotropic compliance matrix and by performing a non-symmetric rotation on it, generate a fully anisotropic compliance matrix. If the rotation is held constant, then by varying the ratio of the Young's moduli, shear moduli, or Poisson's ratios, compliance matrices varying from fully isotropic to fully anisotropic can be generated. For these tests, the following direction cosine matrix was used for the rotation:

$$\begin{bmatrix} .5774 & .5774 & .5774 \\ .7071 & -.7071 & .0000 \\ -.4082 & -.4082 & .8165 \end{bmatrix}$$

Both the ratio of the Young's moduli and the shear moduli were varied over the range of $.1 \leq E_{11}/E_{33} \leq 10$ and $.1 \leq G_{12}/G_{23} \leq 10$. The remaining modulus was set to the average of the other two. While many other schemes for systematically varying the degree of anisotropy could be used, this method appears adequate for this purpose.

4 Numerical Results

The eight node and twenty node hybrid elements were compared to the standard displacement elements for both single elements and for a six element beam. The single elements were tested in pure tension, pure shear, bending, and torsion using both isotropic and anisotropic properties. As is shown in Table I, all elements gave exact solutions for pure tension and pure shear with isotropic material properties. For pure bending, the eight node displacement element is overly stiff but all of the hybrid elements again give exact results. None of the elements is able to give exact results for torsion, but the hybrid elements perform as well or better than the corresponding displacement element.

Table I. Displacements Produced by Cardinal Stress States for Isotropic Material Properties

Element	Pure Tension	Pure Shear	Pure Bending	Pure Torsion
DM 8	100	100	67	84
H8-42	100	100	100	84
H8-18	100	100	100	84
DM 20	100	100	100	95
H20-54	100	100	100	102

As the degree of anisotropy is increased, the ability of the displacement elements decreases. Table II shows the same information as Table I except for anisotropic material properties. Here the ratio of E_{11}/E_{33} is 3 and the material axis is rotated with respect to the element axis by the direction cosines given in the previous section. Both the displacement elements show deterioration in bending and torsion as the degree of anisotropy increases though the degradation is small for the 20 node element.

Table II. Displacements Produced by Cardinal Stress States for Anisotropic Material Properties

Element	Pure Tension	Pure Shear	Pure Bending	Pure Torsion
DM 8	100	100	46	76
H8-42	100	100	100	84
H8-18	100	100	100	84
DM 20	100	100	97	92
H20-54	100	100	100	95

These calculations were performed using double precision for all real variable calculations. The results for the 20 node elements were compared for three integration rules: a $4\times4\times4$, a $3\times3\times3$, and the 14 point rule proposed by Irons [6]. The differences in results were less than 1 percent. Spilker [5] stated that the 14 point rule produced some ill conditioning of H but no such ill conditioning was detected in these runs. Consequently the 14 point rule was used for all subsequent calculations except for occasional checks to assure that the results were indeed the same for the 14 point and $3\times3\times3$ rules.

A six element cantilever beam was analyzed using both eight node and 20 node bricks. These beams are shown in Figure 1. The beams were analyzed both with a pure moment loading and a uniform end shear and for isotropic material properties as well as a series of anisotropic material properties. Figure 2 shows the normalized tip displacement for a pure moment loading with eight node bricks as a function of the degree of anisotropy where the degree of anisotropy is given by the ratio of the Young's moduli in the primary material axes. Figure 3 shows the normalized tip displacement of the cantilever beam for uniform end shear as a function of the degree of anisotropy. The hybrid stress elements are clearly less sensitive to the degree of anisotropy than the displacement. This is true even for the least–order formulations of Punch and Atluri which depend upon element symmetry for their formulation.

Figure 4 shows a comparison of σ_z in the cantilever beam for a pure moment load on the end of the beam as a function of the degree of anisotropy. The stresses in the beam should not change as the material properties change and all stresses except σ_z should be zero. This is clearly not the case for

the displacement elements, even for the 20–node brick. For cases of severe anisotropy, $|\sigma_y|_{max}$ is as much as 93 percent of $|\sigma_y|_{max}$ while the maximum stress of 74 percent of $|\sigma_y|_{max}$. For the 20–node hybrid stress element the corresponding values are 5.6 percent and 3.2 percent. The eight node element actually gives better results than the 20 node brick because the stresses were interpolated at the $2 \times 2 \times 2$ Gauss points which are the optimum points.

The hybrid stress elements clearly give better displacements and stresses for highly anisotropic material properties than their corresponding displacement elements but at some calculational expense. The calculation times are shown in Table III for calculation of the six element cantilever beam. These elements require up to three times as long for the calculations but at least twice as many elements are required to obtain the same degree of accuracy in σ_z and the accuracy in the shear stresses and in σ_x and σ_y is still better in the hybrid stress elements.

Table III. Calculation Time for 6 Element Cantilever Beam

	DM 8	DM 20	H8-18	H8–42	H20–54
Time (sec)	67	552	108	562	1422

5 Conclusions

The hybrid stress elements presented here can provide significantly improved accuracy in both displacements and stresses for highly anisotropic materials in areas of high stress gradients. The 20–node hybrid stress brick element provides increased accuracy over the 20–node displacement element at a cost of approximately a 3 to 1 increase in computation time. The eight node hybrid element H8:18 provides much improved results over the standard eight node displacement element with less than twice the computation time. The most surprising result, however, is that the eight node hybrid element provides almost the same degree of accuracy as the 20 node displacement element at one–fifth of the calculational effort. For high degrees of anisotropy, this element gives superior results to the 20–node displacement element.

Acknowledgment:

The support of this work by the NASA Marshall Space Flight Center under contract NAS 8–37283 and Mr. Larry Kiefling is gratefully acknowledged.

References

1. Spilker, R. C., Maskeri, S. M., and Kania, E., "Plane Isoparametric Hybrid–Stress Elements: Invariance and Optimal Sampling," **Int. J. for Num. Meth. in Engng.**, Vol. 17, pp. 1469–1496, 1981.

2. Spilker, R. L., and Singh, S. P., "Three–Dimensional Hybrid–Stress Isoparametric Quadratic Displacement Elements," **Int. J. for Num. Meth. in Engng.**, Vol. 18, pp. 445–465, 1982.

3. Rubenstein, R., Punch, E. F., and Atluri, S. N., "An Analysis of, and Remedies for, Kinematic Modes in Hybrid–Stress Finite Elements: Selection of Stable, Invariant Stress Fields," **Comp. Meth. in App. Mech. and Engng.**, Vol. 28, pp. 63–92, 1983.

4. Punch, E. F., and Atluri, S. N., "Development and Testing of Stable, Invariant, Isoparametric Curvilinear 2- and 3-D Hybrid–Stress Elements," **Comp. Meth. in App. Mech. and Engng.**, Vol. 47, pp. 331–356, 1984.

5. Punch, E. F., and Atluri, S. N., "Applications of Isoparametric Three–dimensional Hybrid–Stress Finite Elements with Least Order Stress Fields," **Computers & Structures**, Vol. 19 (3), pp. 409–430, 1984.

6. B. M. Irons, "Quadrature Rules for Brick Based Finite Elements," **Int. J. Num. Meth. Engng.**, 3, 293–294, 1971.

7. Pian, T. H. H., and Chen, D. P., "Alternative Ways for Formulation of Hybrid Stress Elements," **Int. J. for Num. Meth. in Engng.**, Vol. 18, pp. 1679–1684, 1982.

8. Pian, T. H. H., and Chen, D. P., "On the Suppression of Zero Energy Deformation Modes," **Int. J. for Num. Meth. in Engng.**, Vol. 19, pp. 1741–1752, 1983.

9. Bathe, K. J., **Finite Element Procedures in Engineering Analysis**, Prentice Hall, New York, 1982.

10. Lekhnitskii, S. G., **Theory of Elasticity of an Anisotropic Elastic Body**, Holden–Day, San Francisco, 1983.

11. Zienkiewicz, O. C., **The Finite Element Method**, 3rd Edition, McGraw–Hill, New York, 1977.

12. Becker, E. B., Carey, G. F., and Oden, J. T., **Finite Elements: An Introduction**, Prentice–Hall, Eaglewood Cliffs, 1981.

13. Atluri, S. N., Gallagher, R. H., and Zienkiewicz, O. C., eds., **Hybrid and Mixed Finite Element Methods**, John Wiley & Sons, New York, 1983.

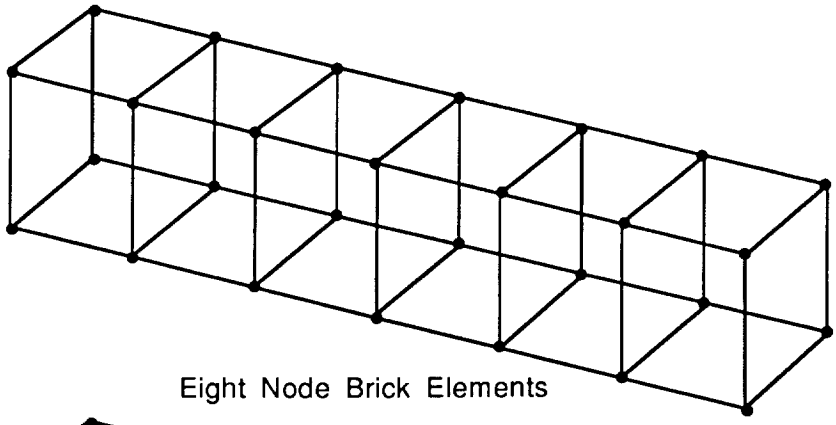

Eight Node Brick Elements

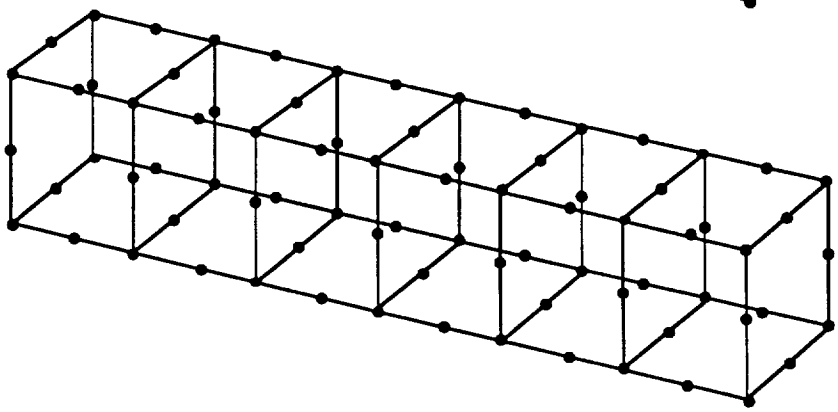

Twenty Node Brick Elements

Fig. 1 Six Element Cantilever Beams

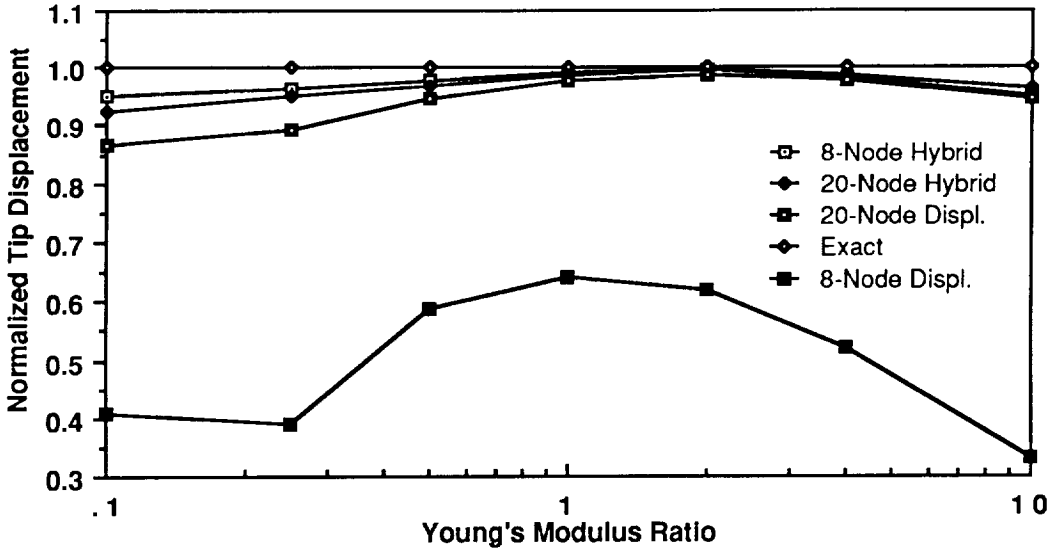

Fig. 2 - Normalized Tip Displacement for Cantilever Beam with Pure Moment Loading

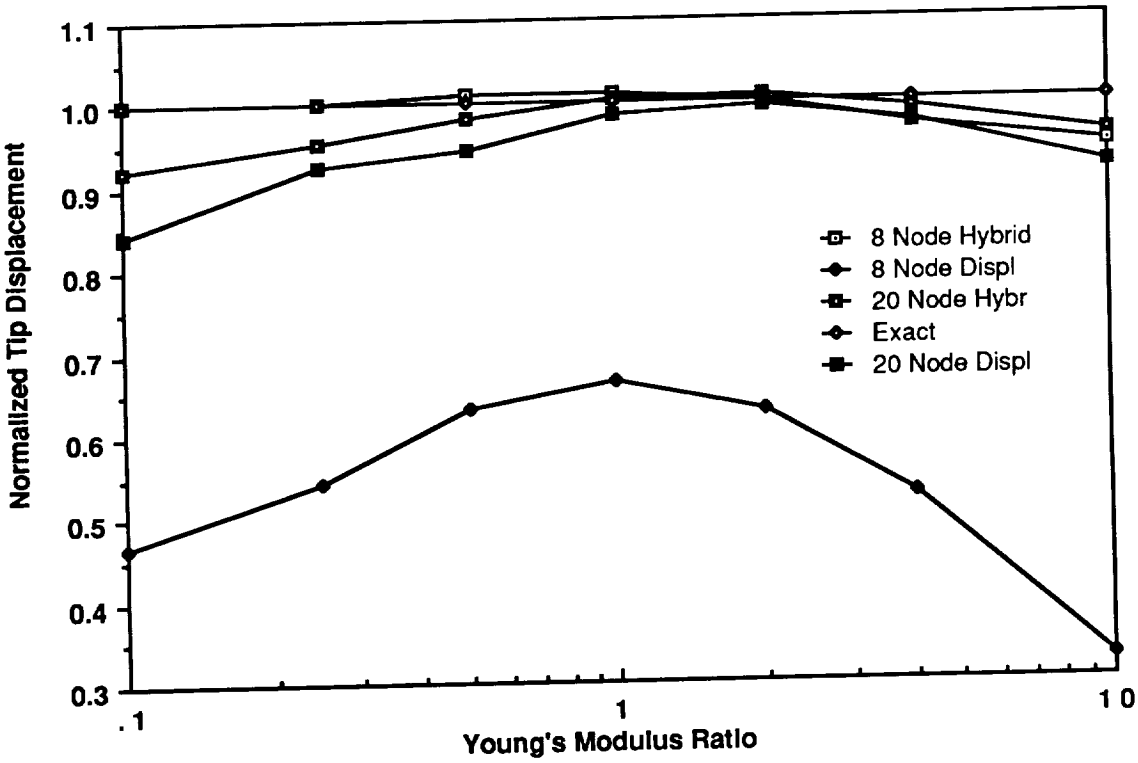

Figure 3 - Normalized Tip Displacement for Cantilever Beam with Uniform End Shear

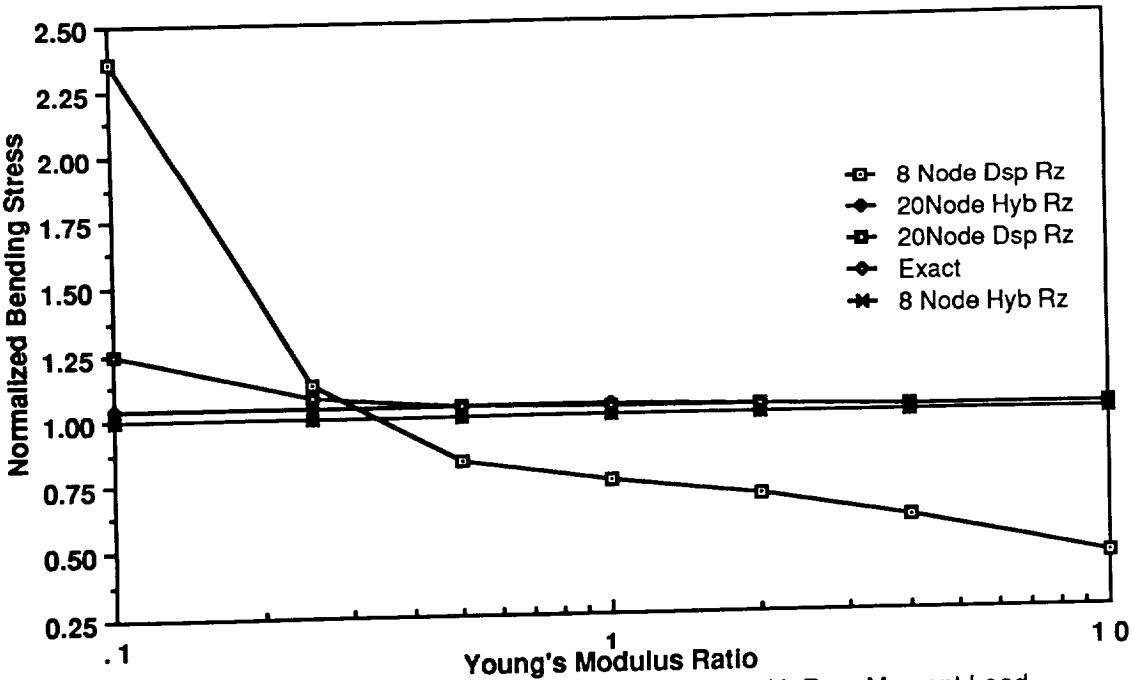

Fig. 4 - Normalized Bending Stress in a Cantilever Beam with Pure Moment Load